

Observation of substitutional and interstitial phosphorus on clean Si(100)-(2×1) with scanning tunneling microscopy

Geoffrey W. Brown,* Blas P. Uberuaga, Holger Grube, and Marilyn E. Hawley

Materials Science and Technology Division, Los Alamos National Laboratory, Los Alamos, New Mexico 87545, USA

Steven R. Schofield,† Neil J. Curson, Michelle Y. Simmons, and Robert G. Clark

Centre for Quantum Computer Technology, School of Physics, University of New South Wales, Sydney, NSW 2052, Australia

(Received 3 June 2005; revised manuscript received 11 August 2005; published 14 November 2005)

We have used scanning tunneling microscopy to identify phosphorus that is present at the clean silicon (100)-(2×1) surface as a result of the thermal cycling necessary for preparation of samples cut from heavily doped wafers. Substitutional phosphorus is observed in top layer sites as buckled Si-P heterodimers. We also observe a second type of feature that appears as a single depressed dimer site. Within this site, the atoms appear as a pair of protrusions in the empty states and a single protrusion in the filled states. These properties are not consistent with known adsorbate signatures or previously reported observations of P-P dimers on the (100)-(2×1) surface. The lack of other impurity sources suggests that they are due to either phosphorus or silicon. The symmetry of the features and their magnitude are consistent with one of those elements residing in an interstitial site just below the top layer of atoms. To identify the type of interstitial, we performed density functional theory calculations for both phosphorus and silicon located below a surface dimer. The resulting charge density plots and simulated STM images are consistent with interstitial phosphorus and not interstitial silicon.

DOI: [10.1103/PhysRevB.72.195323](https://doi.org/10.1103/PhysRevB.72.195323)

PACS number(s): 68.37.Ef, 68.47.Fg, 61.72.Ji

I. INTRODUCTION

The behavior of phosphorus impurities near silicon (100) is important because of its relevance to electronic device processing issues. Detailed, atomic-resolution information about this system has been obtained in the past using scanning tunneling microscopy (STM).^{1–6} STM studies of Si(100)-(2×1) dosed with PH₃ and subsequently annealed to remove hydrogen have elucidated the basic structures of substitutional P and substitutional P-P dimers in these surfaces.^{1–3} Those results provided evidence for surface segregation of P-P dimers from bulk-doped crystals^{4,6} and both P and P-P from epitaxially grown δ -doped layers.^{3,5} The segregation and presence of these species is expected since both are known to play a role in bulk diffusion of phosphorus in silicon.^{7,8} The lack of observation of substitutional P in the bulk-doped crystal work is puzzling since single substitutional phosphorus should diffuse more readily than P-P dimers. In addition, there was no report of interstitial phosphorus, which should be present at some level since it also plays a role in bulk diffusion of phosphorus in silicon. In this paper we report experiments on bulk-doped crystals in which we have observed substitutional P in the Si(100)-(2×1) surface and a second type of feature that we identify as interstitial phosphorus just below the top surface layer of atoms.

II. EXPERIMENT AND SAMPLE PREPARATION

Sample preparation and STM experiments were carried out in an ultrahigh vacuum system with a base pressure of 2×10^{-11} Torr. The silicon samples were rectangles (1.5 mm × 10 mm) cut from 0.5-mm-thick (100)-oriented prime grade wafers that were doped with phosphorus at

$\geq 1 \times 10^{19}/\text{cm}^3$. The samples were handled with ceramic tools and mounted in tantalum/molybdenum/ceramic sample holders to avoid contamination with iron, nickel, or other detrimental transition metals. The samples were prepared by outgassing overnight at 600 °C, followed by a 2 min flash at ~ 1250 °C, a 30 min to 1 h postanneal at ~ 900 °C, and then slow cooling (~ 4 °C/sec) to room temperature. This procedure was necessary to reduce the number of multidimer vacancy defects on the surface of these highly doped samples. For comparison, a second set of samples was prepared using the standard procedure for Si(100)-(2×1),⁹ which does not include the postanneal. During the flash and subsequent heating steps, the chamber pressure remained below 2×10^{-10} Torr. Electrochemically etched platinum iridium alloy (90/10) tips were used for imaging in constant current mode at room temperature.

Figure 1 shows an example of a surface prepared by the standard flash technique, that is, without the postanneal. As shown, even with careful attention to match the temperatures used for lower doped samples, the resulting surface is very defective, having a high density of multidimer vacancies that have lined up in the direction perpendicular to the π -bonded dimer rows on each terrace. This is reported to arise from a combination of stresses induced by the 2×1 reconstruction and P-P dimers at the surface.⁴

In contrast, Fig. 2 shows the surface of a sample from the same wafer that has been prepared using a 30-min-long postanneal as described above. This process is known to allow desorption of P from the surface layer¹⁰ and should also allow rearrangement of the remaining surface vacancies. Here the total density of multidimer vacancy defects is lower and the tendency for the remaining defects to line up has diminished. The fact that the line defects can be eliminated with a

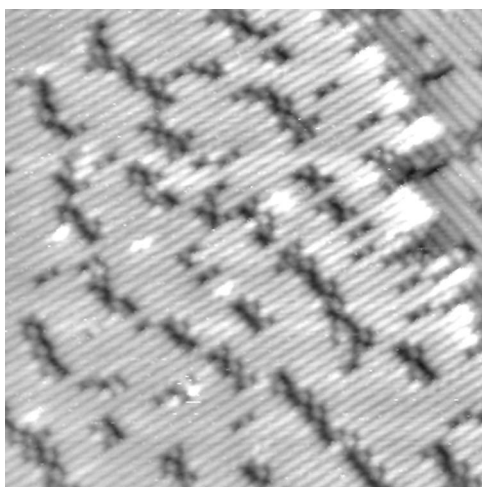


FIG. 1. Filled-state image of a Si(100)- (2×1) surface prepared with the standard flash-anneal technique on a sample cut from a highly doped wafer. Stress due to phosphorus near the surface leads to the vacancy line defects. Several phosphorus-induced features are visible in the clean areas. The image was acquired at -1.25 V sample bias and 400 pA tunnel current. The image area is $350 \text{ \AA} \times 350 \text{ \AA}$.

postanneal is evidence that they are not transition-metal-induced features. Vacancy line defects induced by metal contamination reportedly cannot be eliminated from the surface by annealing.¹¹ Furthermore, the fact that the terrace widths are similar in both cases implies that the primary source of stress in Fig. 1 is the near surface P.¹ The line defects in Fig. 1 are, therefore, related to the high doping level (although the high number of defects present suggests that each one is not associated with an individual phosphorus atom).

III. RESULTS AND DISCUSSION

In addition to vacancies, both Figs. 1 and 2 have examples of two other types of features. In Fig. 2, these are in the areas marked by the circles and can be described initially as “bright” and “dark” features. The empty-state image [Fig. 2(b)] more clearly illustrates their difference with respect to common vacancies, to “C”-type defects identified in early studies of this surface,¹² and to split-off dimer defects¹³ that are all observed in other areas of the image. In general, the bright features are smaller in height and extension than the C defects while the dark features are not as deep as vacancies.

A higher resolution example of one of the asymmetric features from a different sample is shown in the circle in the images in Fig. 3. The feature is asymmetric with respect to the mirror plane of the dimer row and several neighboring dimers in the row are buckled. As noted above, the feature also has a much smaller protrusion in the empty states than do the very obvious C type defects above and below it in the image. Sections through the empty state density of the central part of the feature show it to be $\sim 0.5 \text{ \AA}$ tall at this sample bias compared to the $\sim 1 \text{ \AA}$ tall C defect protrusions. The density of these features is typically less than 1 per $150 \text{ nm} \times 150 \text{ nm}$ area on the postannealed samples,

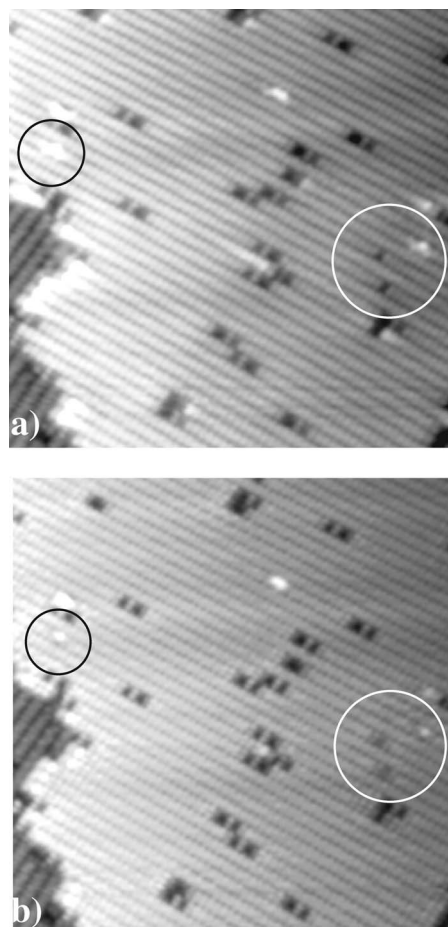


FIG. 2. (a) Filled- and (b) empty-state images of the same area on a Si(100)- (2×1) surface prepared with the standard flash to $\sim 1250 \text{ }^\circ\text{C}$ and a 30 min postanneal at $\sim 900 \text{ }^\circ\text{C}$. The vacancy line defects have diminished due to desorption of phosphorus. The circles mark remaining features that appear to be phosphorus induced. The tunneling conditions were -1.2 V for the filled states, $+1.2$ V for empty states and 150 pA tunnel current in both cases. The image area is $250 \text{ \AA} \times 250 \text{ \AA}$.

but there is some variation within and between samples. This may be due to the uncertainty in the doping level ($\sim 3 \times 10^{19}/\text{cm}^3$).

The symmetry, height, and buckled neighboring dimers of these features are all consistent with what has been observed for P atoms incorporated into Si(100)- (2×1) after a dose-anneal cycle with phosphine.¹⁻³ When the P replaces a Si atom in the top layer, the resulting heterodimer buckles and induces buckling of neighbors along the same row. The assignment of Si-P to these features in our images is also motivated by the observations that phosphorus is expected to be the most common impurity in the sample and that the sample preparation and appearance of these features are also inconsistent with hydrogen or other residual gas impurities in the chamber. Monoatomic hydrogen should not be present since the postanneal temperature is too high for it to remain on the surface. Other gas phase species can also be ruled out because they should occur at lower density, if at all, based on their partial pressures in residual gas analysis. We also do not observe the density of the features to increase in time. One

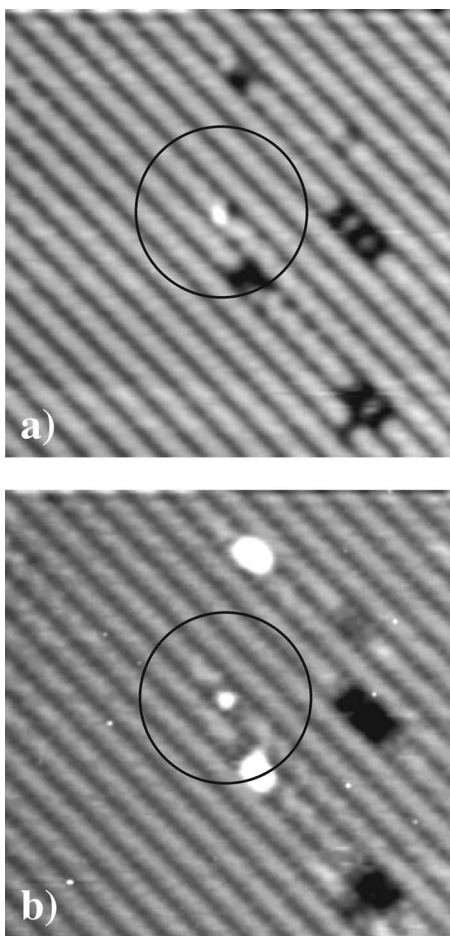


FIG. 3. (a) Filled- and (b) empty-state images from a highly doped sample with one of the “bright” features marked by the circle. A *C* type defect combined with a vacancy is directly below it in the image. The asymmetric dimer and its neighboring structure are consistent with previous observations of Si-P heterodimers. The tunneling conditions were -1.4 V for the filled states, $+1.2$ V for empty states, and 150 pA tunnel current in both cases. The image area is $120 \text{ \AA} \times 120 \text{ \AA}$.

final possibility is that the structures are due to silicon; however, silicon monomers and monovacancies are not stable on these surfaces at room temperature. Given these observations, we identify these bright features as Si-P in the top layer dimer rows resulting from P dopants exposed at, or diffusing to, the surface during the flash or postanneal. This is an interesting result since the P in the heterodimers in our images originates from bulk impurities and not from gas phase dosing of phosphorus-bearing molecules.

An example of one of the dark features is shown in the center of the images in Fig. 4. The specifics of its appearance are weakly tip dependent with small variations in height or symmetry observed from example to example. In general, the features are described as a depressed dimer in both filled and empty states. Specifically in Fig. 4, the depressed dimer in the filled states appears with narrower lateral extent than others on the surface. (We have observed the same details in images in which the tip is able to resolve the dimers in the

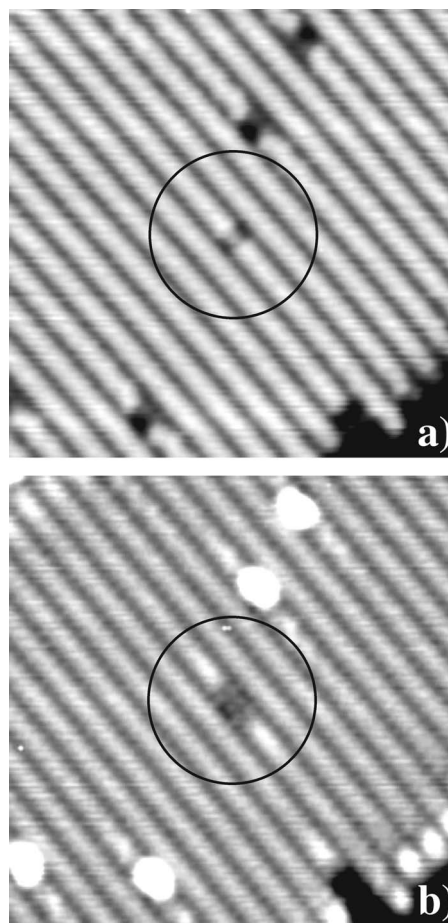


FIG. 4. (a) Filled- and (b) empty-state images of one of the “dark” features observed on the highly doped samples. The tunneling conditions were -1.4 V for the filled states, $+1.0$ V for empty states, and 150 pA tunnel current in both cases. The image area is $120 \text{ \AA} \times 120 \text{ \AA}$.

surface defects, although that is not the case in this image.) In the empty-states image the feature appears as a depressed and resolved dimer (“resolved” implying its appearance as two protrusions). The adjacent dimers in the same row are also resolved. Slight buckling is also present in the depressed dimer, although the lack of buckling in the filled-states image may indicate a tip asymmetry instead. The density of these features is similar to that of the bright features. Finally, the features appear to be charge neutral. We have previously observed charged vacancies on these surfaces¹⁴ and charged phosphorus atoms in substitutional sites beneath Si(100)-(2 × 1) and see a band bending-induced enhancement around either type of feature.¹⁵ That enhancement is not present for the dark features here.

These dark features must also be due to phosphorus or silicon based on the arguments given above concerning other adsorbates or contaminants. These do not appear to be substitutional P-P dimers as seen in another study on hydrogen covered Si(100).⁶ P-P dimers usually appear strongly depressed and resolved in filled state images.^{1,4} We do not see this, even in cases where other features on the surface (defects and step edges) do show resolved dimers. Previous

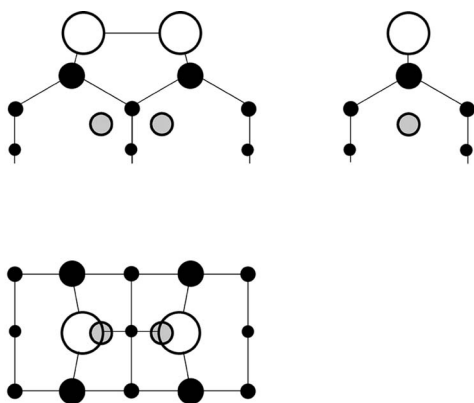


FIG. 5. Schematic diagrams of stable interstitial positions with respect to the surface dimer. The top surface (lower diagram) and side views (upper diagrams) are shown. The empty circles are top layer atoms in dimer rows. The black circles are subsurface atoms whose size diminishes with increasing depth. The gray circles indicate the two possible stable interstitial phosphorus positions. For interstitial silicon, the gray circles would be slightly closer together.

work also reported little corrugation in the empty states images while we consistently image structure in the depression and well resolved adjacent dimers.

At a qualitative level, the features we observe are consistent with what might be expected for an atom in the interstitial space just below a top-surface Si dimer. The structure consists primarily of a single perturbed dimer and does not induce large surface asymmetries. In addition, it creates a depression at the surface in both biases, as might be expected for an interstitial that forms bonds beneath the top layer with the atoms around it. These bonds can cause the top layer atoms to be physically displaced downwards. In addition, bonds created below the surface will lessen the filled- and empty-state orbital density protruding outward from the surface.

The presence of interstitial phosphorus and silicon is expected since both are known to play a role in impurity diffusion in bulk silicon.^{7,8,16} At elevated temperatures, interstitials can be produced and migrate through the crystal. In addition, under certain circumstances, such as high doping, simulations show that phosphorus interstitials can be a major constituent of the phosphorus species.¹⁷

To determine whether the features are due to interstitial phosphorus or silicon, we performed density functional theory calculations with the Vienna *Ab initio* Simulation Package (VASP).^{18–21} A plane wave basis set with an energy cutoff of 255 eV, appropriate for the projector augmented wave pseudopotentials,^{22,23} was used. Si surfaces were modeled by eight layers and a vacuum spacing of 10 Å. A $2 \times 2 \times 1$ Monkhorst-Pack k point mesh²⁴ was used for sampling the Brillouin zone. Initially, the minimum energy structures and total charge densities for interstitial phosphorus and silicon were calculated. Stable configurations occurred when either atom was located between the third and fourth layer of the surface with phosphorus located nearly directly under one of the surface dimer atoms and silicon located closer to the center, but still in an asymmetric position. Since the sur-

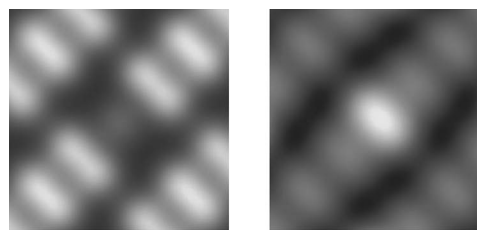


FIG. 6. (Left) Simulated filled-state STM image with phosphorus interstitial located below the center surface dimer. (Right) Simulated filled-state STM image with silicon interstitial located below the center surface dimer. In each case, the charge density was averaged over both possible stable interstitial positions before the STM image was generated.

face dimers can buckle in either direction, there were therefore two stable configurations for each type of atom. Figure 5 schematically illustrates the locations.

To compare with STM data, the charge densities for electrons between 0 eV (the Fermi level) and -3 eV and between 0 eV and -2 eV were considered. Either of these windows roughly corresponds to the states sampled by the tip in the filled-state imaging process. For each window, the charge densities for both interstitial configurations were averaged together to account for the STM tip averaging over the two stable positions. From this data, the method of Tersoff and Hamann²⁵ was used to derive simulated STM images. Once the constant charge density surface was obtained, it was convoluted with box and Gaussian smoothing functions to account for a realistic tip size and shape. The results for the 0 to -3 eV window are shown in Fig. 6. The results for the 0 to -2 eV window were very similar. In each case, the phosphorus interstitial induces a narrowed and depressed dimer and is therefore consistent with the “dark” features in the STM images in Fig. 2. The silicon interstitial induces an enhancement of the top dimer, inconsistent with observations.

Finally, we calculated the barrier for motion between the two interstitial phosphorus configurations using the dimer method.²⁶ The barrier was found to be about 0.7 eV, which, assuming a standard prefactor of $10^{13}/\text{s}$, would imply that the structure flips back and forth every 50 ms at 300 K. The structure appears symmetric since the relatively slow STM imaging process shows the average of the two configurations.

IV. CONCLUSION

In summary, we have identified phosphorus segregated at the surface of Si(100)- (2×1) as a result of the thermal cycling necessary to prepare the samples. Single phosphorus atoms are found in substitutional sites at the surface and we observe the effect of interstitial phosphorus just below the dimer rows. Both features represent single P species in the silicon crystal that have been frozen in at the end of our postanneal step. Since phosphorus primarily desorbs as P_2 at these temperatures,¹⁰ these features represent impurities that had not encountered another of their kind by the time the temperature was lowered. This may explain why we do not

observe P-P dimers in our images. This work also demonstrates an improved method of preparing highly phosphorus-doped silicon samples for scanning tunneling microscopy studies.

ACKNOWLEDGMENT

This work was supported by the U.S. Department of Energy under Contract No. W-7405-ENG-36.

*Electronic address: geoffb@lanl.gov

†Now at School of Mathematical and Physical Sciences, University of Newcastle, Callaghan, NSW 2308, Australia.

- ¹Y. Wang, X. Chen, and R. J. Hamers, *Phys. Rev. B* **50**, 4534 (1994).
- ²L. Kipp, R. D. Bringans, D. Biegelsen, J. E. Northrup, A. Garcia, and L.-E. Swartz, *Phys. Rev. B* **52**, 5843 (1995).
- ³N. J. Curson, S. R. Schofield, M. Y. Simmons, L. Oberbeck, J. L. O'Brien, and R. G. Clark, *Phys. Rev. B* **69**, 195303 (2004).
- ⁴T. Komeda and Y. Nishioka, *Appl. Surf. Sci.* **117/118**, 20 (1997).
- ⁵L. Oberbeck, N. J. Curson, M. Y. Simmons, R. Brenner, A. R. Hamilton, S. R. Schofield, and R. G. Clark, *Appl. Phys. Lett.* **81**, 3197 (2002).
- ⁶Y. Suwa, S. Matsuura, M. Fujimori, S. Heike, T. Onogi, H. Kajiyama, T. Hitosugi, K. Kitazawa, T. Uda, and T. Hashizume, *Phys. Rev. Lett.* **90**, 156101 (2003).
- ⁷P. M. Fahey, P. B. Griffin, and J. D. Plummer, *Rev. Mod. Phys.* **61**, 289 (1989).
- ⁸A. Ural, P. B. Griffin, and J. D. Plummer, *J. Appl. Phys.* **85**, 6440 (1999).
- ⁹B. S. Swartzentruber, Y.-W. Mo, M. B. Webb, and M. G. Lagally, *J. Vac. Sci. Technol. A* **7**, 2901 (1989).
- ¹⁰M. L. Jacobson, M. C. Chiu, and J. E. Crowell, *Langmuir* **14**, 1428 (1998).
- ¹¹J.-Y. Koo, J.-Y. Yi, C. Hwang, D.-H. Kim, S. Lee, and D.-H. Shin, *Phys. Rev. B* **52**, 17269 (1995).
- ¹²R. J. Hamers and U. K. Kohler, *J. Vac. Sci. Technol. A* **7**, 2854 (1989).
- ¹³S. R. Schofield, N. J. Curson, J. L. O'Brien, M. Y. Simmons, R. G. Clark, N. A. Marks, H. F. Wilson, G. W. Brown, and M. E. Hawley, *Phys. Rev. B* **69**, 085312 (2004).
- ¹⁴G. W. Brown, H. Grube, M. E. Hawley, S. R. Schofield, N. J. Curson, M. Y. Simmons, and R. G. Clark, *J. Appl. Phys.* **92**, 820 (2002).
- ¹⁵G. W. Brown, H. Grube, and M. E. Hawley, *Phys. Rev. B* **70**, 121301(R) (2004).
- ¹⁶C. S. Nichols, C. G. Van de Walle, and S. T. Pantelides, *Phys. Rev. B* **40**, 5484 (1989).
- ¹⁷M. Uematsu, *J. Appl. Phys.* **82**, 2228 (1997).
- ¹⁸G. Kresse and J. Hafner, *Phys. Rev. B* **47**, R558 (1993).
- ¹⁹G. Kresse and J. Hafner, *Phys. Rev. B* **49**, 14251 (1994).
- ²⁰G. Kresse and J. Furthmüller, *Comput. Mater. Sci.* **6**, 16 (1996).
- ²¹G. Kresse and J. Furthmüller, *Phys. Rev. B* **54**, 11169 (1996).
- ²²P. E. Blöchl, *Phys. Rev. B* **50**, 17953 (1994).
- ²³G. Kresse and D. Joubert, *Phys. Rev. B* **59**, 1758 (1999).
- ²⁴H. J. Monkhorst and J. D. Pack, *Phys. Rev. B* **13**, 5188 (1976).
- ²⁵J. Tersoff and D. R. Hamann, *Phys. Rev. Lett.* **50**, 1998 (1983).
- ²⁶G. Henkelman and H. J. Jónsson, *J. Chem. Phys.* **111**, 7010 (1999).